Corrosion Characteristics in Weld Heat-affected Zone of Al-Zn-Mg Alloy†

Toshio KURODA*, Shinya KANAMITSU and Toshio ENJO*****

Abstract

Relation between pitting potential and microstructure in weld heat-affected zone (HAZ) of a commercial Al-Zn-Mg alloy (7NO1-T6 alloy) was investigated by means of resistivity measurement, transmission electron microscopy and anodic polarization measurement in 1M NaCl solution. As the specimens solution-treated at 653K were aged at 483K and 523K for various times, the resistivity change due to the precipitation of η' phase and η phase was related to the pitting potential in anodic polarization measurement.

As the 7NO1-T6 alloy was heated at various temperatures for 60 sec, the pitting potential also decreased with increasing heating temperature. This result means that the pitting potential increased with decreasing solute concentration of Zn and Mg in the matrix.

The specimen was welded by using DCSP TIG welding procedure in helium gas at the heat input of 2300 KJ/m. The resistivity measurement was carried out by using isochronal annealing technique for the specimen in each part of the HAZ. The resistivity in the region at 0-25 mm from the bond region was higher than that of base metal(T6), and the solute concentration of Zn and Mg in the region was high. The pitting potential in each part of the HAZ was also measured, and the potential in the region of 0-25 mm away from the bond region was lower than that of base metal.

KEY WORDS : (Al-Zn-Mg Alloy) (HAZ) (Pitting Potential) (Electrical Resistivity) (Transmission Electron Microscopy)

1. Introduction

Weldable Al-Zn-Mg alloys have been widely used for various structures such as railway vehicles. As the structures were overhauled at a constant period, the stress corrosion cracking and corrosion were found out. To be clarify this cause is very important for the suppression of the accidents of this structure.

The aging of the alloy follows the precipitation sequence: G. P. zones → η' intermediate phase → η stable phase ($MgZn_2$)[1-3].

The specimen consisting of G. P. zones and η' precipitates has very high susceptibility to stress corrosion cracking[4,5]. The specimen consisting of η phase has low susceptibility to stress corrosion cracking. It was reported that the initiation behavior of the pitting, that is important to be related to stress corrosion cracking, depended on the concentration of Zn and Mg in the matrix[6].In the previous report[7], the microstructure change in the weld heat-affected zone of Al-Mg-Si alloy(6063-T5) could be evaluated by the resistivity value related to the concentration of Mg in the matrix using electrical resistivity measurement. Then, the relation between the resistivity and the pitting potential in the Al-Zn-Mg alloy was measured. The microstructure change in the weld heat-affected zone was evaluated by the resistivity change, and the relation between resistivity and pitting potential was clarified.

2. Experimental Procedure

The material used in this investigation was Al-Zn-Mg series 7NO1-T6 alloy with 12 mm thickness. The chemical compositions are shown in **Table 1**. The heat treatment in this alloy was carried out using salt bath. Namely, the specimens were solution-treated at 653K for 7.2ks, water quenched, and then artifical aged at 483K and 523K for various times in the salt bath. Bead on plate welding by DCSP TIG using helium gas was carried out.

The solution or precipitation behavior of the preci-

Table 1 Chemical compositions of material used (mass%)

Material	Zn	Mg	Cu	Si	Fe	Mn	Cr	Ti	Zr	Al
7NO1	4.58	1.15	tr.	0.08	0.16	0.45	0.21	0.05	0.2	Bal.

† Received on May 7, 1990
* Instructor
** Graduate student
*** Professor (Deceased)

Transactions of JWRI is published by Welding Research Institute of Osaka University, Ibaraki, Osaka 567, Japan

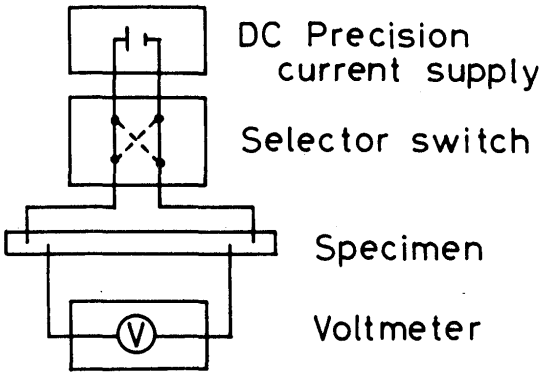

Fig. 1 Schematic illustration of electrical resistivity measurement by conventional potentiometric method.

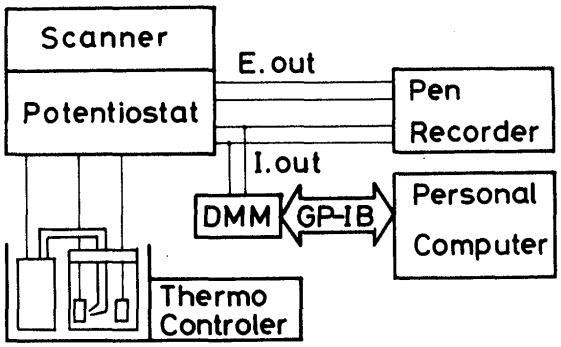

Fig. 2 System diagrams of anodic polarization measurement by potentiostat.

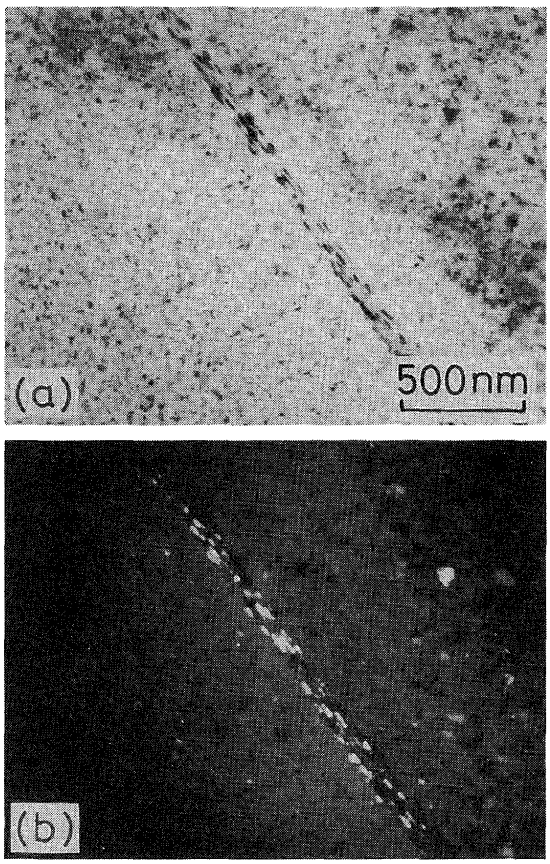

Fig. 3 Transmission electron micrographs of 7NO1-T6 base metal.
(a) Bright field image, (b) Dark field image

pitates and relatively insoluble compounds was measured by means of transmission electron microscopy and electrical resistivity measurement. The specimen for electrical resistivity measurement was cut off in the size of 2 mm wide, 0.5 mm thick by using electro discharge machine. The electrical resistivity measurement was made by conventional potentiometric method as shown in **Figure. 1**. The electrochemical measurement was made in order to evaluate the corrosion resistance. Anodic polarization curves showing the relation of potential to current density, were developed for each specimen. Each specimen was polished mechanically, first 1500 grit emery paper, and finally on a cloth with 1 micron grain diamond abrasive. And the specimen was rinsed in deionized water, degresed in acetone, and then masked along its edges with stop-off lacquer prior to testing.

Each curve was developed by anodically polarizing a specimen from its free corrosion potential to a potential above its pitting potential as shown in **Figure. 2**. Potential/current curves were recorded at potential scan rate of 0.33V/sec. The potential and current were also measured automatically using a computer which was connected with a potentiostat using G.P.I.B. interface. The pitting potential was exactly decided on the basis of the digital data from the computer. The electrolyte used was 1M NaCl solution which was deaerated by bubbling argon throught the solution for at least 1.8 ks, before immersing the specimen. pH of the electrolyte was 11.0.

3. Results and Discussion

3.1 Relation between microstructure and pitting potential

Figure 3 shows transmission electron micrographs of the 7NO1-T6 alloy. Grain boundary precipitates, η' phase and G.P. zones in the matrix can be observed[8]. The grain boundary precipitates was confirmed η phase by the analysis of electron diffraction pattern. The dark field image is shown in Fig. 3-(b). The grain boundary precipitates was η' phase and η phase precipitates a little in the matrix.

Figure 4 shows transmission electron micrographs, as the 7NO1-T6 alloy was solution-treated at 653K for 7.2ks and then aged at 483K and 523K. In case of aging at 483K, the precipitation free zone(PFZ)[9,10] at the grain boundary was present and fine precipitates were also

present. G.P. zones are hardly observed. In case of aging at 523K, as shown in Fig. 4-(b), η phase precipitates at the grain boundary, and PFZ can be observed at the grain boundary. In these case, the aging treatments at 483K and 523K cause the precipitation of η phase, η' precipitates and PFZ. The 7NO1-T6 alloy was solution-treated at 653K for 7.2ks, the precipitates such as Fig. 3 were hardly observed, and it means that η' precipitates and η phase were solutionized in the matrix. The precipitation amounts of the precipitates was evaluated by the resistivity change by using electrical resistivity measurement in previous report[7]. Then in this study, the relation between resistivity change and pitting potential was discussed.

Figure 5 shows a relation between pitting potential and resistivity change, as the 7NO1-T6 alloy was solution-treated at 653K for 7.2ks, water quenched, and then aged at 483K and 523K for various times. This pitting potential was decided in the anode polarization curve as same as the previous report[6]. The resistivity decreased with increasing aging time and reached a constant value as shown in subdiagram in Fig. 5. This phanomena is considered to be related to the decrease of the concentration of Zn and Mg in the matrix in solution. The resistivity change $\Delta\rho$ indicates the difference between the value ρ_0 at solution treatment and ρ_t after aging at 483K and 523K for various times. The increase of the

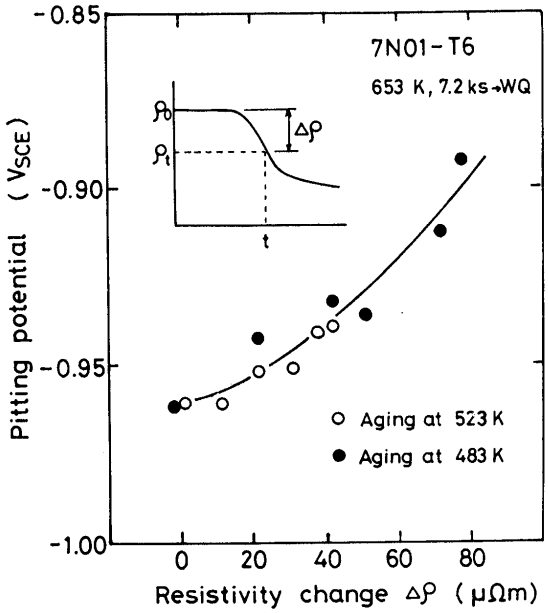

Fig. 5 Relation between pitting potential and resistivity change.

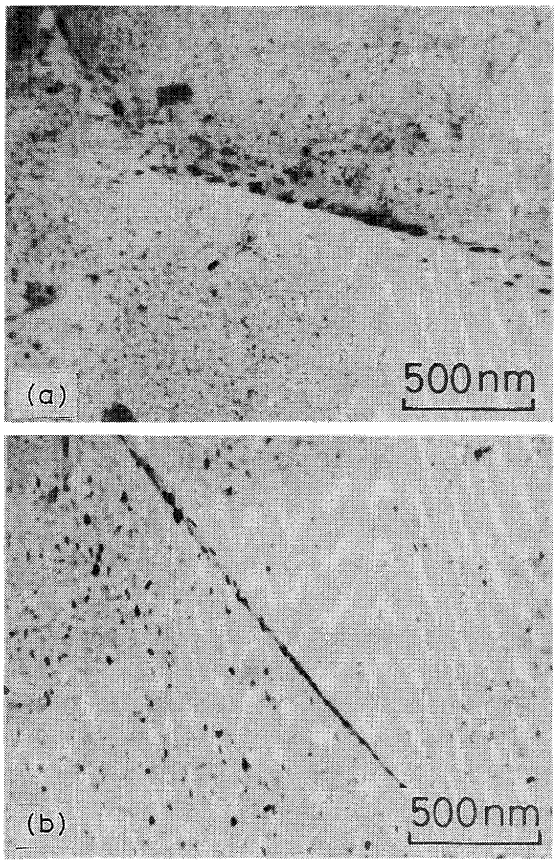

Fig. 4 Transmission electron micrographs of 7NO1 alloy aged at 483K(a) and 523K(b) for 7.2ks after solution treatment at 653K for 7.2ks.

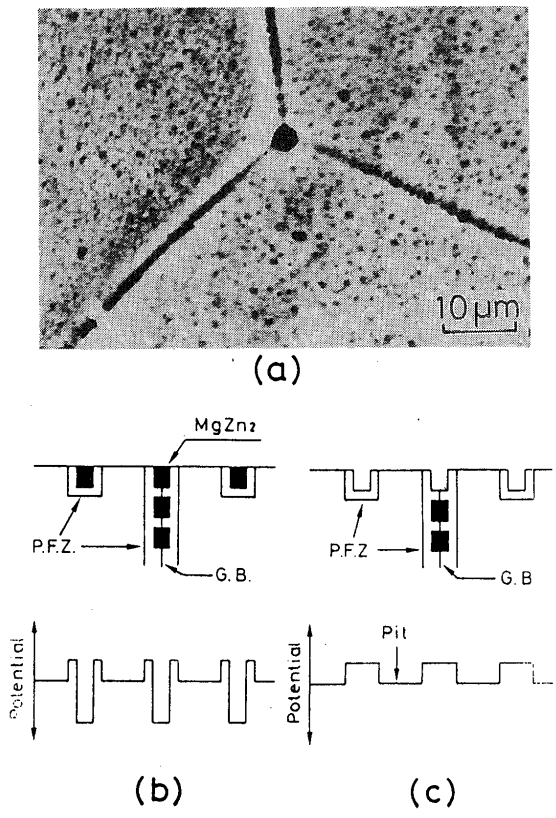

Fig. 6 Surface morphology after immersion for 3.6ks in 1M NaCl solution (a) and schematic illustration of the potential near the surface(b),(c).

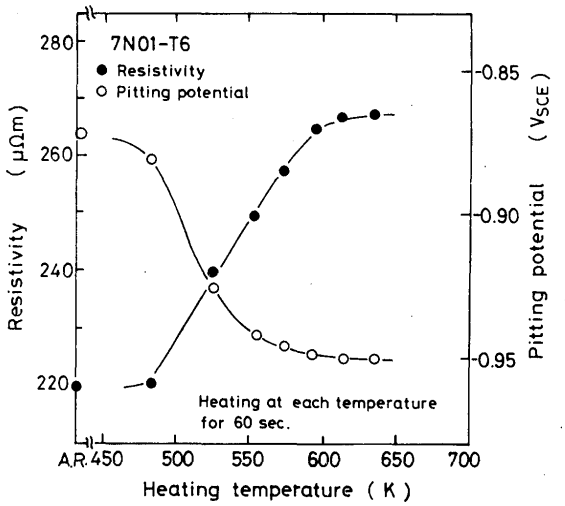

Fig. 7 Relation between resistivity and heating temperature, as the 7NO1-T6 alloy was heated at each temperature for 60 sec.

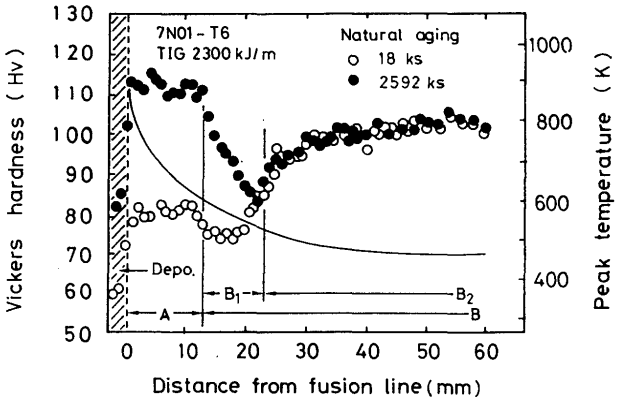

Fig. 8 Hardness distribution in the weld heat-affected zone of 7NO1-T6 alloy.

$\Delta\rho$ is due to the precipitation of η' precipitates and η phase as shown in Fig. 4. Namely, it is related to the decrease of the concentration of Zn and Mg in solution in the matrix by the precipitation of η' precipitates and η phase. The pitting potential increases a little with increasing resistivity change up to 20 $\mu\Omega$m. Above the value, the pitting potential decreased drastically with increasing resistivity change. It means that the decrease of the precipitation amount of η' precipitates and η phase by aging treatment causes the increase of the pitting potential. That is, the concentration of the Zn and Mg in solution in the matrix decreases with increasing precipitation amount by aging treatment, and the pitting potential increases with decreasing concentration of Mg and Zn in solution in the matrix. The resistivity change and pitting potential has good relationship.

Figure 6 indicates the surface morphology after immersion for 3.6ks in 1M NaCl solution(a) and schematic illustration of the potential near the surface(b) , (c), as the 7NO1-T6 alloy was solution-treated at 653K for 7.2ks, water quenched, and then aged at 523K for 7.2ks. The intergranular and transgranular corrosion were observed. Based on the microstructure in Fig. 4-(b), the grain boundary precipitates and precipitates in grain such as η phase, or the region near the precipitates were considered to be corroded selectively. This phenomena shows Fig. 6-(b), (c). In this alloy, zinc of 5% and magnesium of 1.5% were added. The addition of Mg up to 5% affects a little the pitting potential. The addition of Zn causes the decrease of the passive range[11]. Zn greatly reduces the pitting potential[11]. Therefore its addition will reduce the passive range usually observed in aluminum alloys. The addition of 5% Zn reduces 200mV$_{SCE}$. It is also important to note that the most common grain boundary precipitates $MgZn_2$ is easily dissolved at potentials above $-860mV_{SHE}$ ($-1100mV_{SCE}$)[14]. Consequently, as shown in Fig. 6-(b), as the specimen was immersed in the 1M NaCl solution, $MgZn_2$ at the grain boundary and η phase in grain has low potential, and then the precipitates are considered to be corroded selectively. But, the matrix near the precipitates has high pitting potential, and is hardly corroded, as a result, the increase of the current hardly generates.

Generally, the precipitation free zone has poor Mg and Zn content[1], the pitting potential is higher than that of the matrix, and difficult to be corroded. $MgZn_2$ was corroded out after the immersion, the pitting potential of the matrix between precipitates becomes lowest. Then, it is considered that pits generate in the matrix. Consequently, the precipitations of η phase and η' precipitates cause the decrease of the concentration of Zn and Mg in solution, and cause the increase of the pitting potential.

3.2 Pitting potential in weld heat-affected zone

As the 7NO1-T6 alloy was welded, the various regions were heated at various temperatures in the weld heat-affected zone[8,13-15].

Figure 7 indicates a relation between resistivity and pitting potential as the specimens were heated at various temperatures for 60 sec.

In case of T6 base metal(AR) consisting of G.P. zones and η' precipitates, the resistivity is 200 $\mu\Omega$m and very low. The resistivity of the specimen heated at 483K is same as that of T6 base metal. In the temperature range up to 573K, the resistivity decreases with increasing heating temperature. This means that G.P. zones, η' precipitates and η phase are partially solutionized in the matrix. And the pitting potential also decreases with increasing heating temperature. The decrease of the pitting potential depends on the solution amount of Zn

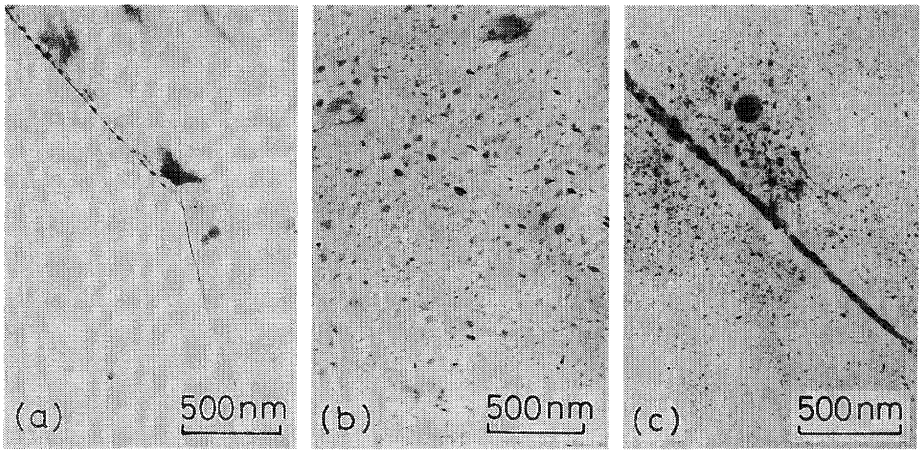

(a) 5mm from fusion line (b) 20 mm from fusion line (c) 35 mm from fusion line

Fig. 9 Transmission electron micrographs in the HAZ of 7NO1-T6 alloy welds.

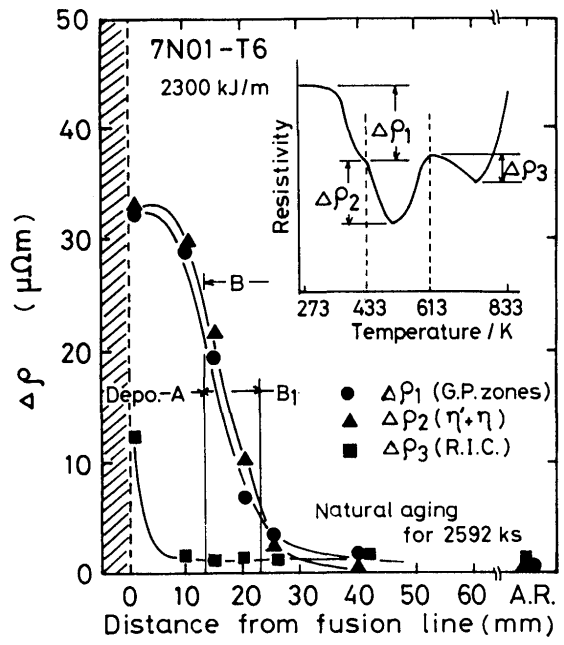

Fig. 10 Distribution of electrical resistivity change in TIG welds of 7NO1-T6 alloy.

involving the solution of G.P. zones, η' precipitates and η phase. Above 600K, the resistivity becomes high and constant, this means that η' precipitates and η phase were solution-treated. The pitting potential is also constant.

Figure 8 indicates the distribution of hardness in the weld heat-affected zone, as the sample 7NO1-T6 alloy was welded at the heat input of 2300 kJ/m. The hardness of T6 base metal was Hv103. The hardness in the region A is Hv80 after welding. But, the hardness increases Hv115 by the natural aging at room temperature for 2592ks after welding. This increase of the hardness is due to the formation of G.P. zones. The hardness in the B_1 region is Hv80 and low as same as that of the region A. But, the hardness increses by natural aging after welding. But, the increment of hardness increases with becoming near the weld bond. The hardness in the B_2 region is about constant, and hardly affected by the welding heat. The distribution of hardness depends on the distribution of the precipitates such as G.P. znes, η' precipitates and η phase.

Figure 9 shows transmission electron micrographs in the heat-affected zones of 7NO1-T6 alloy welds. The grain boundary precipitates, η phase and fine G.P. zones in the grain are observed at the area 5 mm from fusion line in the region A. At the area 20 mm from fusion line in the region B_1, large sizes of η phase are obsered. At the area 35 mm from fusion line in the region B_2, grain boundary precipitates and η phase in grain are present. The microstructure change, as the 7NO1-T6 alloy was welded, agrees with that of the report by Mizuno et. al[8].

Figure 10 indicates the change in resistivity, as the 7NO1-T6 alloy was heated for 600 sec at each temperature up to 833K respectively, namely isochronal annealed. The resistivity can be devided by $\Delta\rho_1$ related to G.P. zones, $\Delta\rho_2$ related to $\eta' + \eta$ precipitates and $\Delta\rho_3$ related to relatively insoluble compounds. The relatively insoluble compounds such as $Al_{18}Cr_2Mg_3$ were formed during casting and solution treatment[7], because of the addition of various minor elements such as Cr, Mn, Fe, Si so on. Concerning $\Delta\rho_1$ and $\Delta\rho_2$, it was confirmed that $\Delta\rho_1$ increases with increasing G.P. zones in the sample prior isochronal annealing. $\Delta\rho_2$ decreases with increasing $\eta' + \eta$ precipitates in the sample prior isochronal annealing. Consequently, that $\Delta\rho_1$ and $\Delta\rho_2$ are high in the region A means that η phase and η' precipitates are solutionized by during welding and G.P.

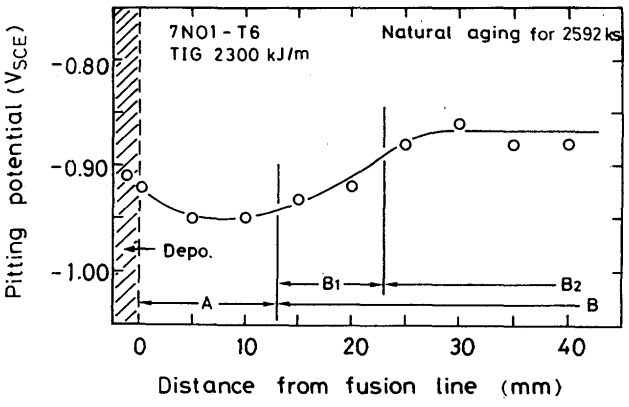

Fig. 11 Distribution of pitting potential in TIG welds of 7NO1-T6 alloy.

zones form during natural aging after welding. It means that the concentration of Zn and Mg in solution is high. In case of B_1 region, $\Delta\rho_1$ and $\Delta\rho_2$ increase with reaching toward weld fusion line. This means that G.P. zones, η' precipitates and η phase are partially solutionized and the concentration of Zn and Mg in solution increased, and G.P. zones formed during natural aging after welding. In case of B_2 region of 28 mm from fusion line, $\Delta\rho_1$ and $\Delta\rho_2$ are very small, and it means that G.P. zones and η' precipitates were hardly solutionized during welding. The pitting potential is affected by the amount of η' precipitates and η phase.

Figure 11 indicates the change in pitting potential in the weld heat-affected zones of 7NO1-T6 alloy welds. The pitting potential in the B_2 region is high and constant, because that the resistivity hardly change as shown in Fig. 10. The pitting potential in the B_1 region decreased with reaching to the fusion line, and this phanomena corresponds to the resistivity change as shown in Fig. 10.

In the region A, η' precipitates, η phase were solutionized and the concentration of Mg and Zn is highest, as shown in Fig. 10, and the pitting potential is lowest. This region A is called solution treatment region of precipitates. The pitting potential is highest at the bond area in the region A. It is considered that the relatively insoluble compounds such as $Al_{18}Cr_2Mg_3$ were partially solutionized and the concentration of Cr in solution in the matrix increased[6], because Cr causes the increase of the pitting potential. Consequently, the pitting potential considered to be high in the area near the fusion line.

4. Conclusion

Relation between pitting potential and microstructure in weld heat-affected zone of a commercial Al-Zn-Mg alloy (7NO1-T6) was investigated by means of resistivity measurement, transmission electron microscopy and anodic polarization measurement. The results obtained in this investigation are summarized as follows.

(1) As the specimens solution-treated at 653K were aged at 483K and 523K for various times, the resistivity change due to the precipitation of η' precipitates and η phase has good relationships to pitting potential in anodic polarization measurement.

(2) As the 7NO1-T6 alloy was isochronal annealed at various temperatures for 60 sec, the resistivity increased and the pitting potential decreased with increasing heating temperature. This means that the pitting potential is related to the concentration of Zn and Mg in solution in the matrix.

(3) The resistivity measurement was carried out by using isochronal annealing technique for the specimen in each part of the HAZ, that was made by using DCSP TIG welding procedure. For the region at 0-25 mm from weld fusion line, it was confirmed that η' precipitates, η phase were fully solutionized by means of transmission electron microscopy, and the resistivity was higher than that of the base metal (T6). The pitting potential in the region were also lower than that of the base metal. Consequently, the pitting potential has a good relationship to electrical resistivity.

References

1) J. D. Embury and R. B. Nicholson: Acta Metall., 13-4, (1965), 403.
2) G. Thomas and J. Nutting: J. Inst. Metals, 88, (1959,60), 81.
3) T. Enjo and T. Kuroda: J. Soc. Mater. Soc. Japan, 29-321, (1980), 617 (In Japanese).
4) P. K. Poulose, J. E. Morral and A. J. McEvily: Metall. Trans., 5, (1974), 1393.
5) M. Miyamoto and Y. Murakami: J. Japan Inst. Metals, 37, (1969), 394 (in Japanese).
6) T. Enjo, T. Kuroda and S. Kanamitsu: J. High Temp. Soc., 12-4, (1986), 163 (In Japanese).
7) T. Enjo and T. Kuroda: J. Japan Weld. Soc., 51-2, (1982), 168 (In Japanese).
8) M. Kikuchi and M. Mizuno: J. Light Metals Soc., 28-7, (1987), 728 (In Japanese).
9) K. G. Kent: J. Inst. Metals, 97, (1969), 127.
10) A. J. Sedriks, P. W. Alattery and E. N. Pough: Trans. ASM, 62, (1969), 238.
11) I. L. Muller and J. R. Galvele: Corrosion Sci., 17, (1977), 995.
12) W. W. Binger, E. H. Hollingtwooth and D. D. Sprowls: Aluminium (Kent R. Von Van Horn, ed), 1, ASM, (1967), 209.
13) S. Sugiyama and T. Fukui: J. Japan Weld. Soc., 35, (1966), 790.
14) J. H. Rogerson: Brit. Weld. J., 11, (1964), 12.
15) M. Mizuno, M. Kikuchi, Y. Baba and T. Fukui: J. Japan Light Metal Soc., 26, (1976), 564 (In Japanese).
16) Y. Baba and A. Takashima: J. Japan Light Metal Soc., 24-5, (1974), 216 (In Japanese).